Power System Technology
ISSN:1000-3673

Received: 06-01-2025 Revised: 15-02-2025 Accepted: 25-03-2025

Estimation of Global Solar Radiation (GSR) using Seven Meteorological Parameters at Eastern Hill, Okhaldhunga, Nepal

Basanta Kumar Rajbanshi[1], Ram Gopal Singh[2], Narayan Basnet[3], Sanjay Kharel[4], Sourav Rijal[3], Bed Raj KC[5], Usha Joshi[6]

[1.] Research Scholar, Shri Ramswaroop Memorial University (SRMU), Devaroad-Lucknow, Barabanki, India

basantaraz22@gmail.com, basantaraz05@gmail.com , ORCID ID: 0009-0003-7953-7475

[2.] Dean, Faculty of Physical Sciences, Shri Ramswaroop Memorial University (SRMU), Devaroad-Lucknow, Barabanki, India

dean.phy@srmu.ac.in

[3.] Research Scholar, Patan Multiple Campus, Tribhuvan University, Kathmandu, Nepal

narayan.basnet1740@gmail.com, saurabrijal35@gmail.com

[4.] Research Scholar, Central Department of Physics, Tribhuvan University, Kathmandu, Nepal

kharelsanjay620@gmail.com

[5.] Vice Chancellor, Pokhara University, Gandaki Province, Nepal

bedrajkc@yahoo.com

[6.] Campus Chief, Patan Multiple Campus, Lalitpur, Kathmandu, Nepal

usha.joshi@pmc.tu.edu.np

**Corresponding author: (E-mail: basantaraz05@gmail.com, basantaraz22@gmail.com)*

Abstract

For developing solar energy technologies, an in-depth knowledge of the distribution of solar radiation in every geographic region is important. Using seven meteorological parameters-highest and lowest temperatures, precipitation, solar radiation, maximum and minimum humidity, and wind speed, this study used RadEst 3.0 to estimate daily GSR in Okhaldhunga, (27.31°N, 86.50°E, 1731 m) Nepal for 2021-2023. Four models; Bristow and Campbell (BC), Campbell and Donatelli (CD), Donatelli and Bellocchi (DB), and Donatelli-Campbell-Bristow-Bellocchi (DCBB) are utilized to estimate the radiation.

Power System Technology
ISSN:1000-3673
Received: 06-01-2025 Revised: 15-02-2025 Accepted: 25-03-2025

The models were evaluated using statistical methods such as coefficient of determination (R^2), mean bias error (MBE), mean percentage error (MPE), mean bias error (MBE), and root mean square error (RMSE). Parameter fitting (PF) calibrates all four models by maximizing R^2 and minimizing CRM, and RMSE. In 2021, 2022, and 2023, the yearly average GSR was 14.6 ± 0.27 MJ/m^2/day, 15.5 ± 0.27 MJ/m^2/day and 15.4 ± 0.32 MJ/m^2/day respectively. The highest GSR values were recorded in 2023 at 29.6 MJ/m^2/day, with a total yearly GSR of 5618 MJ/m^2. CD model had the highest R^2 values for all three years, so it is the best model for estimating GSR in this region.

Keywords: meteorological parameters; statistical methods; pyranometer; global solar radiation; RadEst 3.0 software; atmospheric transmissivity

1. Introduction

Nepal's topography is diverse, featuring mountains of varying heights that make up its geomorphology. The country is situated in a region that receives abundant solar energy. Nepal is a relatively small country with a total land area of 147,516 square km, approximately 800 km long and 200 km wide. Nepal is located between latitudes 26°22' and 30°27' N and longitudes 80°4' to 88°12' E. Nepal is surrounded by the territories of China and India. Thanks to its diverse climate and rich biodiversity, Nepal's varying climate is noticeable every 200 meters above sea level. However, the country's reserves of fossil fuels, such as coal, oil, and gas, remain inaccessible. The main cause of Nepal's economic and social underdevelopment is the lack of energy supplies.

According to the Solar and Wind Energy Resource Assessment (SWERA) conducted by the Alternative Energy Promotion Centre (AEPC), Nepal has an economic potential for on-grid solar PV installations of up to 2,100 MW. As of 2022, there were 974,000 installed home solar PV systems, with the majority located in isolated regions of Western Nepal with poor connectivity to the national grid [1].

In the fiscal year 2017–18, the breakdown of energy consumption was as follows: 2.2% from renewable sources, 27.8% from conventional sources, and 70% from commercial sources. The most used traditional energy source is firewood, but its use leads to waste and deforestation. Additionally, open fires contribute to indoor air pollution, which poses a significant health risk. Lamsal's 2019 study found that 22% of Nepalese, primarily in rural regions, lack access to electricity [2]. During the dry season, businesses, industries, and households face prolonged power outages, lasting several hours each day. The public, private families, and the business and industrial sectors lack awareness of the financial and environmental benefits of energy efficiency. There are no industry standards for energy-efficient lighting, household products, and advancements in industry.

Power System Technology
ISSN:1000-3673
Received: 06-01-2025 Revised: 15-02-2025 Accepted: 25-03-2025

Fuel sales increased by 10.87% overall in 2021. Diesel sales went up by 12.6%, kerosene by 21.61%, and LPG by 6.19%. However, sales of Alternative Technology Fuels (ATF) plummeted by 65.32%. In 2022, petrol sales surged by 40.43%, nearly doubling in value. Similarly, sales values of ATF, LPG, and diesel increased by 32.24%, 11.5%, and 74.55%, respectively. Meanwhile, sales of paraffin dropped by 4.99%[1].

Solar radiation is a safe and clean energy source. Nepal annually experiences an average of 3.6 to 6.2 kWh/m^2/day of solar insolation. According to Shrestha et al. (2003), Nepal has 300 bright days and 6.8 hours of sunshine per day, indicating a significant potential for free and clean solar energy [3]. The current annual average GSR is 4.23 kWh/m^2/day, as stated by Poudyal (2015)[4]. Nepal falls within one of the most beneficial insolation zones on the global map. Therefore, utilizing solar energy is considered one of the best solutions to address the energy crisis in developing Asian countries like Nepal[5,6]. With a few different equations of varying degrees of complexity and the representative work of Ångström, the Global Solar GSR can be easily estimated from the measured sunshine hours and other meteorological parameters [7,8].

Ali M. A. et al. conducted research on artificial neural network optimization to accurately predict GSR and compared the results with traditional techniques [9]. To estimate the GSR for North-West Nigeria, Olomiyesan et al. analyzed the performance of four models. A comparison of the four new models with the established Garika, Samani and Hargreaves models was conducted using monthly meteorological data on temperature, sunlight hours, and GSR[10]. Nage examined multiple models based on Ethiopia's temperature and sunshine hours[11]. Haushan Li et al. proposed a new model based on the Hargreaves and Samani (HS) technique to compute GSR at 65 stations in China[12]. The monthly global sun radiation over twelve main Libyan towns was estimated by Teyabeen, A. et al[13].

Hassan et al. evaluated twenty models, including seventeen new ones, based on ambient temperature. For estimating GSR for Egypt, the three remaining models are Allen's model (Allen 1997), Goodin et al. (1999), and Annandale et al. (2002)[14]. In Pakistan, K A Narejo et al. used newly developed equations simulated by MEP to estimate solar radiation for the ASHRAE constant. They computed three forms of radiation using these new constants: GSR, beam solar radiation (BSR), and diffuse solar radiation (DSR) for five distinct cities across the globe, including Karachi, London, New York, Sydney, and Tokyo[15].

In Morocco, North Africa, Hissou, H., et al. investigated a novel machine-learning technique for calculating solar radiation[16]. Using several empirical models, Joshi et al. calculated GSR for Khumaltar and Kathmandu, Nepal[17]. Dhakal et al. looked at several empirical models based on machine learning, artificial neural networks, and temperature to compute GSR at Biratnagar, Nepal[18]. Joshi et al. used the RadEst 3.0 program to estimate the daily solar radiation flow within the Western upland area of Simikot, Nepal[19].

Power System Technology
ISSN:1000-3673
Received: 06-01-2025 Revised: 15-02-2025 Accepted: 25-03-2025

Bristow and Campbell found a connection between near-surface air temperature and the atmosphere's ability to transmit radiation during the daytime. This model has been enhanced over the years and has been applied in several studies. They adjusted the models by including a correction factor that accounts for the seasonal variations in the mid-latitude region. This concept was later used in the development of weather generators[20]. Donatelli and Bellocchi (2001) and Donatelli et al. (2003) attempted to improve the consideration of seasonal variations in different areas [21,22]. Poudyal et al. calculated the GSR for Kathmandu, Nepal for the years 2005 and 2007 using the RadEst 3.0 program [23]. Similarly, GSR was computed at Simara Airport in Nepal [24]. Based on data from 2011 and 2013 Chhetri and Gurung in Jumla, Nepal, used the RadEst 3.00 program to compute the GSR[25].

This study focuses on examining the spatial distribution of solar energy across Nepal, a nation with abundant yet underutilized solar resources. Utilizing local meteorological data and advanced modelling techniques, the research accurately evaluates GSR levels. By analyzing various models, the study identifies the most effective approach for predicting solar radiation in Okhaldhunga. The results provide valuable insights to support strategic planning for future solar energy projects and promote the sustainable development of renewable energy in Nepal.

2. Theoretical Formulation of RadEst 3.0 software

To calculate a region's GSR, it is necessary to gather high-quality data from comprehensive radiation observations across all main climatic zones. Several empirical formulas have been proposed to determine the daily GSR at different sites worldwide based on various characteristics. One of the potential choices for estimating daily GSR is the RadEst 3.0 program, which utilizes maximum and minimum temperatures in its calculations.

The work presents the RadEst 3.0 software, which can estimate daily GSR data using parameters such as wind speed, precipitation, temperature, humidity, and geographic location. The research aims to identify the optimal model for the relationship between GSR, temperature, and rainfall to support the development of solar energy technology in Nepal and similar geographical areas. RadEst 3.0 software was selected for its reliability, user-friendliness, and suitability for a wide range of applications, leveraging readily available meteorological data from stations worldwide.

The RadEst 3.00 program is a collaboration between ISCI-Crop Science and FAO-SDRN-Agrometeorology Group. It allows the daily estimation of GSR at a specific location using four basic models. The results can be evaluated using graphical and statistical methods.

Power System Technology
ISSN:1000-3673
Received: 06-01-2025 Revised: 15-02-2025 Accepted: 25-03-2025

Models:

The study used the CD, BC, DB, and DCBB models. These models calculate the daily solar radiation at the Earth's surface. They utilize specific parameters to generate results within statistical tools.

tt_i = estimated transmissivity,

τ = clear sky transmissivity,

ΔT = monthly average temperature,

T_{max} =daily maximum air temperature,

T_{min} = daily minimum air temperature,

b = coefficient of temperature range

c = very sensitive empirical parameter,

T_{nc} = temperature factor,

c_1 = seasonal variation magnitude parameter,

c_2 = seasonal variation profile parameter,

i = day of the year, i = 1 to 365 or 366

$f(T_{avg})$ = average temperature function,

$f(T_{min})$ = minimum temperature function.

Est Rad_i = estimated radiation (MJ m^{-2} day^{-1})

PotRad_i = Potential radiation outside the atmosphere (MJ m^{-2} day^{-1})

These models calculate the atmospheric transmissivity of solar radiation by using the difference between the maximum and minimum air temperatures. The estimated value of radiation (Est Radi) is obtained by multiplying the value of potential radiation (Pot Rad_i) outside the earth's atmosphere by the estimated transmissivity (tt_i).

$$Est\ Rad_i = tt_i\ Pot\ Rad_i$$

$$\text{Pot Red}_{doy} = 117.5 dd_2 \frac{h_s \text{Sin(lat) Sin(dec)+Cos(lat) Sin}(h_s)}{\pi} \quad (1)$$

This formula uses lat to represent the monitoring site's latitude in degrees, dec for solar declination, dd2 for the sun's distance, and h_s for half-day length.

Power System Technology
ISSN:1000-3673
Received: 06-01-2025 Revised: 15-02-2025 Accepted: 25-03-2025

2.1 BC Model

The original BC model, which served as the basis for subsequent models, estimates the daily radiation flux of incoming solar radiation by using the link between the GSR load and the diurnal air temperature range. More clouds (transmissivity) mean less sunlight reaching the ground, causing lower daytime temperatures. Nighttime temperatures will be influenced by cloud cover as well. On the other hand, the clear sky will result in higher minimum and maximum air temperatures because of increased transmissivity and higher intake of short-wave radiation. This approach has been applied to several projects over the past many years, and advancements have also been produced. Estimated transmissivity is

$$tt_i = \tau\left[1 - \exp\left(\frac{-b\,\Delta T_i^c}{\text{month}\,\Delta T}\right)\right] \quad \ldots (2)$$

Hence from the equation estimated radiation provided by

$$\text{Est Red}_i = \tau\left[1 - \exp\left(\frac{-b\,\Delta T_i^c}{\text{month}\,\Delta T}\right)\right]\text{PotRed}_i$$

(3)

Where,

$$\Delta T_i = T_{max_i} - \frac{T_{min_i} + T_{min(i+j)}}{2}$$

(4)

2.2 CD Model

The CD model is based on the BC model and accounts for seasonality impacts in mid-latitude regions like Nepal by using a correction factor. This correction factor, known as the summer night temperature factor (T_{nc}), increases the estimated transmissivity. In this model, transitivity is obtained as,

$$tt_i = \tau\left[1 - \exp\left\{-b \times f\left(T_{avg}\right)\Delta T_i^2\, f(T_{min})\right\}\right]$$

(5)

Thus,

$$\text{Est Red}_i = \tau\left[1 - \exp\left\{-b \times f\left(T_{avg}\right)\Delta T_i^2\, f_1(T_{min})\,\text{PotRed}_i\right\}\right]$$

(6)

Where,

$$T_{avg} = \frac{T_{max_i} + T_{min_i}}{2}$$

(7)

Power System Technology
ISSN:1000-3673
Received: 06-01-2025 Revised: 15-02-2025 Accepted: 25-03-2025

2.3 DB Model

DB model, known as the third model, estimates the total solar energy from air temperature. Unlike previous models, this model considers the variation of transmissivity under clear skies. It also uses additional parameters c_1 and c_2 to represent seasonality variables and estimate the temperature difference. The transmissivity in the DB model is obtained as,

$$tt_i = \tau\left[1 + f(i)\left[1 - \exp\left\{\frac{-b\,\Delta T^2}{\Delta T_{week}}\right\}\right]\right] \quad (8)$$

Providing radiation estimates as,

$$EstRed_i = \tau\left[1 + f(i)\left[1 - \exp\left\{\frac{-b\,\Delta T_i^2}{\Delta T_{week}}\right\}\right]\right] PotRed_i \quad (9)$$

Where,

$$f(i) = c_1\left[\sin\left(i\,c_2\frac{\pi}{180}\right) + \cos\left\{i\,f(c_2)\frac{\pi}{180}\right\}\right] \quad (10)$$

$$f(c_2) = 1 - 1.90\,c_3 + 3.83c_3^2 \quad (11)$$

$$c_3 = c_2 \text{ integer } (c_2) \quad (12)$$

2.4 DCBB Model

This is the fourth model built using atmospheric air fluctuation data. Each of the three models in this set has an on/off switch for every feature. To provide more details, let's consider setting the parameter c_1 to 0. When the option to display the average monthly temperature change (ΔT) is selected and T_{nc} is unchecked, the BC model replaces the DCBB model. The estimated transmissivity is,

$$tt_i = \tau\left[1 + f(i)\left[1 - \exp\left\{\frac{-b\,\Delta T^2 f(T_{min})}{\Delta T_{avg}}\right\}\right]\right] \quad (13)$$

Which provides radiation estimates as,

$$EstRed_i = \tau\left[1 + f(i)\left[1 - \exp\left\{\frac{-b\,\Delta T_i^2 f(T_{min})}{\Delta T_{avg}}\right\}\right]\right] PotRed_i \quad (14)$$

Power System Technology
ISSN:1000-3673
Received: 06-01-2025 Revised: 15-02-2025 Accepted: 25-03-2025

Where,

$$f(i) = c_1\left[\sin\left(i\, c_2 \frac{\pi}{180}\right) + \cos\left\{i\, f(c_2)\frac{\pi}{180}\right\}\right] \quad (15)$$

$$f(c_2) = 1 - 1.90\, c_3 + 3.83 c_3^2 \quad (16)$$

$$f(T_{avg}) = 0.017 \exp\left\{\exp\left(-0.053 \times T_{avg}\right)\right\} \quad (17)$$

Where,

$$T_{avg} = \frac{T_{max_i} + T_{min_i}}{2} \quad (18)$$

$$f(T_{min}) = \exp\frac{T_{min}}{T_{nc}} \quad (19)$$

$c_3 = c_2$ integer (c_2)

3 Methods and instrumentation

3.1 Site selection

Nepal is in a region that is favourable for solar energy. Okhaldhunga, geographically situated 1839.3 meters above sea level, experiences dry winters and a temperate highland tropical climate. The mean yearly temperature is 18.11ºC, which is -3.89% colder than the national average. Okhaldhunga has 207 rainy days and averages 263.0 mm of precipitation yearly. The wettest, coldest, driest, and hottest months are January (2.44ºC), July (851.46mm), June (26.05ºC), and December (10.0mm) respectively. There are 206.89 days with rainfall (≥ 1.0 mm) and 158.11 days without rain. The region has an average humidity of 66.64%.

3.2 Instrument

Meteorological factors such as solar radiation, maximum and minimum temperatures, rainfall, humidity, and wind speed are used as input for the models. The Department of Hydrology and Meteorology (DHM/GoN) provided the data for these parameters for 2021, 2022, and 2023 in Okhaldhunga. Rainfall is measured using a Udometer, while temperature is measured using a maximum-minimum thermometer. The CMP6 Pyranometer is utilized to measure GSR. This device operates based on the thermocouple concept, where radiation is converted directly into a temperature difference, resulting in a voltage difference. The data logger then reads this voltage to determine radiation intensity in units of w/m^2. The device is

Power System Technology
ISSN:1000-3673
Received: 06-01-2025 Revised: 15-02-2025 Accepted: 25-03-2025

designed to function in a temperature range of -40 to 80 0C and has a wide spectral range of 310 nm to 2800 nm[19].

3.3 File format

The input file is in ASCII format with no headers. It contains eight variables in a DAT file (Golden Software/Surfer 2019) with space separation. These variables represent model data for a single year (from 1 to 365), including rainfall (mm), maximum temperature (°C), minimum temperature (°C), GSR (MJ/m^2/day), maximum humidity (%), minimum humidity (%), and wind speed (m/s). The daily GSR values have been estimated for 2021, 2022, and 2023 using input data from Okhaldhunga, Nepal.

3.4 Input format

The latitude, longitude, and altitude of the given location are first set using the RadEst 3.00 software. Additionally, clear sky transmissivity values should be set between 0.6 and 0.8. The latitude is used in calculating the estimated radiation, and clear sky transmissivity is used to calculate the atmosphere's transmissivity coefficient.

3.5 Analysis

The ASCII-formatted file is opened with latitude, longitude, and altitude information. Parameter fitting (PF) and auto-optimization (AO) are used in different models. To compare and calculate GSR, at least two years of data are required. AO is less precise compared to PF. The key factors are closely related to solar radiation-influencing factors. In PF, various parameters are adjusted to ensure that measured and estimated radiation have equivalent mean values. Graphical analysis is used to compare the estimated radiation value derived from measurements with actual radiation levels. Throughout this process, various statistical tools such as the coefficient of determination (R^2), mean bias error (MBE), mean percentage error (MPE), mean error (ME), root mean square error (RMSE), coefficient of residual mass (CRM), correlation coefficient (r), and coefficient of variation (CV) are used. These tools support the models in evaluating and comparing the data.

4 Results and discussion

The performance of each model is tested through auto-optimization, and the estimated GSR it produces differs significantly from the measured GSR. Next, using parameter fitting (PF) based on data from Okhaldhunga in 2021, all four models are calibrated to maximize the coefficient of determination (R^2) and minimize RMSE and CRM. Table 1 presents the modelled and measured estimated average value, maximum, and annual total value of the GSR of Okhaldhunga for AO and PF in 2021. It is found that the average annual value of GSR is 14.6 MJ/m^2/day. The CD model has a value almost identical to that of other models.

Power System Technology
ISSN:1000-3673
Received: 06-01-2025 Revised: 15-02-2025 Accepted: 25-03-2025

The GSR for the data from 2022 and 2023 is estimated using the calibrated values of the parameter from 2021. Measured and estimated GSR values are very similar. Tables 2 and 3 provide the parameter fitting-based testing values for 2022 and 2023.

The measured and model-estimated average value, maximum value, and yearly total value of GSR for model CD are nearly identical in Tables 1, 2, and 3 when compared to the other three models. Thus, in 2021, 2022, and 2023, model CD provides more accurate estimates of GSR in hilly altitude zones than the other three models. The seasonal variation of the GSR for 2021, 2022, and 2023 is displayed in Figure 6. The highest GSR values are recorded during the spring months (17.40 ± 0.61 MJ/m^2/day, 18.06 ± 0.55 MJ/m^2/day, and 17.77 ± 0.84 MJ/m^2/day for the years 2021, 2022, and 2023, respectively) due to clear skies after the rainy season. Conversely, minimal GSR levels are observed during the autumn of 2023 (13.53 ± 0.49 MJ/m^2/day) and the winter months (13.27 ± 0.33 MJ/m^2/day, 13.52 ± 0.40 MJ/m^2/day) for the years 2021 and 2022, respectively, due to cloud cover sky and rainfall.

Throughout all three years, except 2023, the seasons with the highest and lowest solar radiation flux are spring and winter, respectively. This is due to the lower relative humidity, reduced cloud cover, less rainfall, and absence of wind during spring, resulting in a higher flux of solar radiation than in summer and winter. The highest radiation levels are observed after the monsoon rains in June, July, and August, when the sky is clear.

The monthly variance of GSR for 2021, 2022, and 2023 is displayed in Figure 7. The highest GSR occurs in April for the year 2021 (20.17 ± 0.88 MJ/m^2/day), in March for the year 2022 (19.14 ± 0.81 MJ/m^2/day), and in May for the year 2023 (20.27 ± 1.42 MJ/m^2/day) due to clear skies after the rainy season. Conversely, due to cloud cover and rainfall, the lowest GSR occurs in August 2021 (11.43 ± 0.89 MJ/m^2/day), January 2022 (12.14 ± 0.61 MJ/m2/day), and August 2023 (10.39 ± 0.85 MJ/m^2/day). Over the three years, the GSR trend remains largely stable. The error bars, based on standard deviation, indicate the variation in GSR for a given month.

The variation in seasonal precipitation for the years 2021, 2022, and 2023 can be seen in Figure 8. In 2023, the highest and lowest rainfall will occur during the summer, with 1286.55 mm, and in the winter, with 2.62 mm, respectively. Similarly, Figure 9 displays the seasonal fluctuation in average wind speed for the years 2021, 2022, and 2023. The highest average wind speed (1.4403 m/s) occurs in the spring of 2023, while the lowest average wind speed (0.5829 m/s) occurs during the summer of the same year.

In 2021, 2022, and 2023, the strongest radiation days are April 23 (29.0294 MJ/m^2/day), August 11 (29.5404 MJ/m^2/day), and May 5 (29.5734 MJ/m^2/day) respectively. The least intense days of the year for 2021, 2022, and 2023 are October 19 (1.1926 MJ/m^2/day), June 29 (2.2955 MJ/m^2/day), and August 13 (2.8366 MJ/m^2/day) respectively. The highest

Power System Technology
ISSN:1000-3673
Received: 06-01-2025 Revised: 15-02-2025 Accepted: 25-03-2025

temperature days of the year for 2021, 2022, and 2023 are October 15 (29.4°C), August 17 (28.9°C), and June 9 (32.5°C) respectively. Similarly, the lowest temperature days of the year for 2021, 2022, and 2023 are December 31 (4.0°C), January 28 (2°C), and January 19 (3.6°C) respectively. In 2021, the greatest rainfall day was July 15 with 94.6 mm of rain. In 2022, the greatest rainfall day was July 2 with 79.4 mm of rain. In 2023, the greatest rainfall day was August 25 with 97.6 mm of rain. As for the maximum wind speeds, in 2021 it was recorded on April 24 at 2.2616 m/s, in 2022 on April 15 at 3.7008 m/s, and in 2023 on February 25 at 9.9716 m/s.

4.1 Error analysis

Tables 4, 5, and 6 display the statistical error comparing measured and estimated GSR for 2021, 2022, and 2023 respectively. The correlation coefficient and coefficient of determination (R^2) in these tables are both relatively modest. Specifically, in 2021 (i.e., R^2 = 0.59), 2022 (i.e., R^2 = 0.54), and 2023 (i.e., R^2 = 0.59), the values are higher for modular CD. Furthermore, for the CD model in all three years, there are relatively small values of RMSE, mean bias error (MBE), mean percentage error (MPE), and coefficient of residual mass (CRM). This indicates that, among all the models, the CD model is the best for this location.

Figs. 1, 2, and 3 show the linear variation of the daily measured and projected GSR for the four models provided for the years 2021, 2022, and 2023. The graphs illustrate the consistent agreement between the estimated and daily measured GSR for all models. The value of R^2 in the CD model is higher than in the other models for all three years, indicating better agreement. Once again, across all models, 2021 and 2023 demonstrate greater agreement than 2022. The R^2 values for the CD model in 2021, 2022, and 2023 are 59%, 54%, and 59% respectively. This difference can be attributed to rainfall and the regional climate."

The transmission coefficients for 2021, 2022, and 2023 can be found in Figures 4a, 4b, and 4c, respectively. After rain, the sky clears up, which increases transmittance. Figures 5a, 5b, and 5c illustrate the daily variation of observed radiation and the multiple of potential radiation and transmissivity, indicating the high amount of GSR accessible in the research area. Even during the winter, Okhaldhunga experiences a narrow zenith angle, low radiation, and high transmissivity. In the summer months, there is considerably less GSR observed due to more rainfall, gloomy skies in June, July, and August, and strong wind speeds. However, it is currently an extremely hot season. The sky clears when it rains, resulting in a high radiation flux during autumn.

The total amount of rainfall in 2021 was 1838.6 mm, which was higher than in 2023 (1740.19 mm) and 2022 (1488.85 mm). During the summer, there are high temperatures and increased rainfall, which reduces the GSR. Generally, the GSR trend increases in June, July, and August and decreases in December. However, because it depends on temperature and

Power System Technology
ISSN:1000-3673
Received: 06-01-2025 Revised: 15-02-2025 Accepted: 25-03-2025

precipitation, the GSR trend varies. GSR is lower in June, July, and August due to cloud cover and rain. Precipitation and GSR are negatively correlated and a positive correlation between temperature and GSR.

The GSR in Jumla, a mid-hill area, is higher than that of Simikot, a high-altitude mountain region (6648 MJ/m^2/day for 2013 and 7309 MJ/m^2/day for 2011). The BC model is better suited for Jumla than Simikot. The GSR is higher in the spring and fall for Simikot, whereas it is higher in the spring for Jumla. This difference is attributed to changes in altitude and local weather [25].

Although Simikot is at a higher altitude, Jumla records greater solar radiation. This discrepancy is likely due to Jumla experiencing clearer skies and reduced cloud cover, which allows more sunlight to reach the surface directly. Seasonal variations, especially during spring when the sun is more directly overhead, could further contribute to Jumla's higher GSR. Moreover, variations in measurement locations and methodologies might also impact the recorded data, emphasizing that solar radiation patterns can differ significantly across regions.

Table 1 Measured and model estimated average GSR, maximum GSR and total GSR for the year 2021 at Okhaldhunga

Model	Average GSR (MJ/m^2 /day)			Maximum GSR (MJ/m^2 /day)			Total GSR (MJ/m^2)		
	AO	Mea	PF	AO	Mea	PF	AO	Mea	PF
BC	14.3	14.6	14.6	23.9	29.0	24.2	5217	5340	5328
CD	14.4	14.6	14.6	23.8	29.0	23.9	5251	5340	5313
DB	14.2	14.6	14.6	22.7	29.0	23.1	5179	5340	5338
DCBB	13.2	14.6	14.6	21.4	29.0	23.2	4811	5340	5316

Table 2 Measured, and model estimated average GSR, maximum GSR and total GSR for the year 2022 at Okhaldhunga

Model	Average GSR (MJ/m^2 /day)			Maximum GSR (MJ/m^2 /day)			Total GSR (MJ/m^2)		
	AO	Mea	PF	AO	Mea	PF	AO	Mea	PF
BC	15.1	15.5	14.6	24.4	29.5	23.9	5516	5675	532

Power System Technology
ISSN:1000-3673
Received: 06-01-2025 Revised: 15-02-2025 Accepted: 25-03-2025

									5
CD	14.9	15.5	14.5	23.9	29.5	23.6	5452	5675	5308
DB	14.9	15.5	14.6	22.0	29.5	22.8	5443	5675	5331
DCBB	14.0	15.5	14.6	24.1	29.5	24.6	5118	5675	5332

Table 3 Measured and model estimated average GSR, maximum GSR and total GSR for the year 2023 at Okhaldhunga

Model	Average GSR (MJ/m^2/day)			Maximum GSR (MJ/m^2/day)			Total GSR (MJ/m^2)		
	AO	Mea	PF	AO	Mea	PF	AO	Mea	PF
BC	15.0	15.4	15.0	26.3	29.6	26.2	5492	5618	5471
CD	15.5	15.4	15.3	27.0	29.6	26.8	5667	5618	5587
DB	14.8	15.4	15.0	25.7	29.6	24.7	5420	5618	5482
DCBB	15.5	15.4	14.9	26.3	29.6	26.9	5649	5618	5438

Table 4 Statistical Error for the year 2021 for Okhaldhunga

Model	MBE (MJ/m^2/day)	RMSE(MJ/m^2/day)	MPE (%)	r	CRM (MJ/m^2/day)	R^2	ME	CV
BC	-0.032748	3.70	-5.7316	0.711179	0.00	0.51	0.47	25.31
CD	-0.073599	3.31	-4.7942	0.769307	0.01	0.59	0.57	22.63
DB	-0.006212	3.43	-6.8224	0.739850	0.00	0.55	0.54	23.47
DCB	-0.066244	4.00	-7.1782	0.64820	0.00	0.4	0.38	27.3

Power System Technology
ISSN:1000-3673
Received: 06-01-2025 Revised: 15-02-2025 Accepted: 25-03-2025

B				**3**		**2**		**3**

Table 5 Statistical Error for the year 2022 for Okhaldhunga

Model	MBE ($MJ/m^2/day$)	RMSE ($MJ/m^2/day$)	MPE (%)	r	CRM ($MJ/m^2/day$)	R^2	ME	CV
BC	**-0.95762**	**3.98**	**1.7192**	**0.690024**	**0.06**	**0.48**	**0.42**	**25.61**
CD	**-1.00462**	**3.72**	**2.4010**	**0.733560**	**0.06**	**0.54**	**0.50**	**23.93**
DB	**-0.94189**	**3.99**	**0.5496**	**0.675670**	**0.06**	**0.46**	**0.42**	**25.65**
DCBB	**-0.93885**	**4.31**	**0.3866**	**0.623887**	**0.06**	**0.39**	**0.32**	**27.70**

Table 6 Statistical Error for the year 2023 for Okhaldhunga

Model	MBE ($MJ/m^2/day$)	RMSE ($MJ/m^2/day$)	MPE (%)	r	CRM ($MJ/m^2/day$)	R^2	ME	CV
BC	**-0.403326**	**3.99**	**-2.9970**	**0.721144**	**0.03**	**0.52**	**0.50**	**25.93**
CD	**-0.083036**	**3.70**	**-3.9209**	**0.767154**	**0.01**	**0.59**	**0.57**	**24.01**
DB	**-0.370832**	**3.95**	**-4.0997**	**0.718489**	**0.02**	**0.52**	**0.51**	**25.66**
DCBB	**-0.492991**	**4.73**	**-5.1346**	**0.582523**	**0.03**	**0.34**	**0.30**	**30.71**

Power System Technology
ISSN:1000-3673

Received: 06-01-2025 Revised: 15-02-2025 Accepted: 25-03-2025

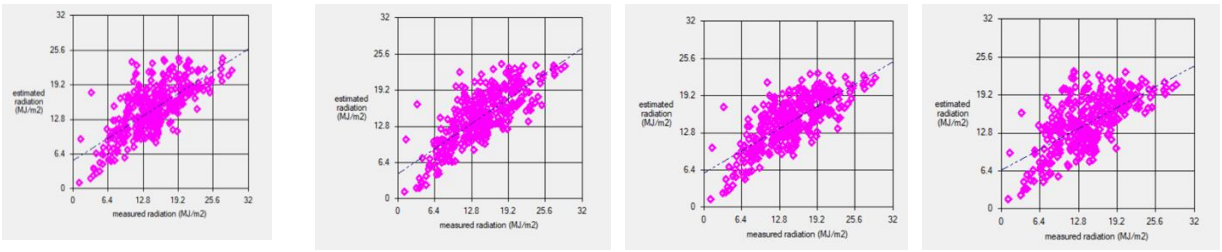

BC 2021 **CD 2021** **DB 2021** **DCBB 2021**

Fig. 1 Linear relationship analysis of measured and estimated GSR data for Okhaldhunga in 2021.

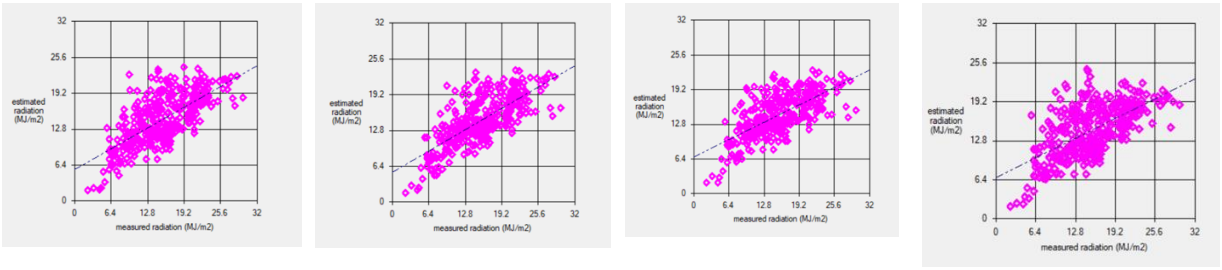

BC 2022 **CD 2022** **DB 2022** **DCBB 2022**

Fig. 2 Linear relationship analysis of measured and estimated GSR data for Okhaldhunga in 2022

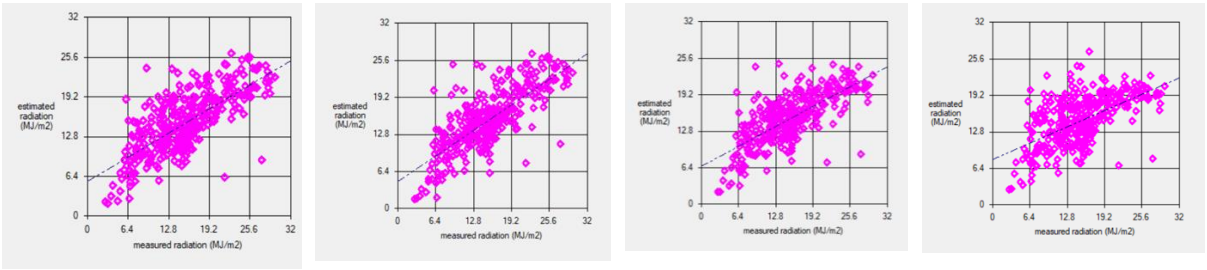

BC 2023 **CD 2023** **DB 2023** **DCBB 2023**

Fig. 3 Linear relationship analysis of measured and estimated GSR data for Okhaldhunga in 2023

…

Power System Technology
ISSN:1000-3673

Received: 06-01-2025 Revised: 15-02-2025 Accepted: 25-03-2025

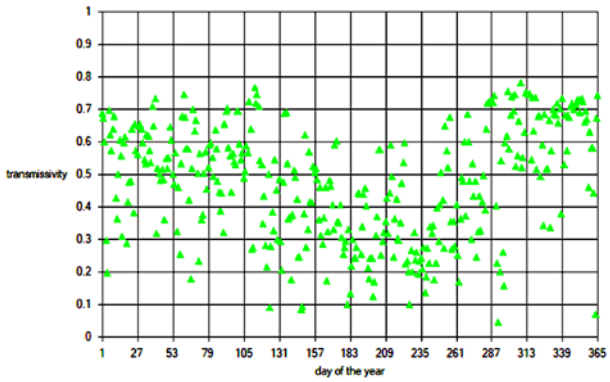

4 a. Daily Transmissivity coefficient 2021

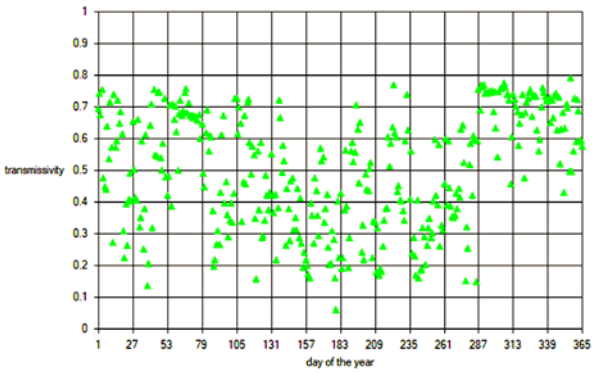

4 b. Daily Transmissivity coefficient 2022

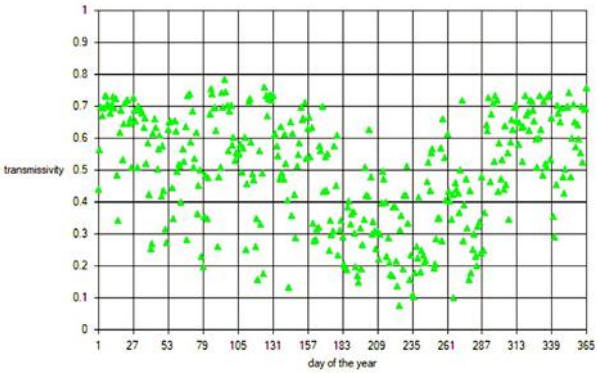

4 c. Daily Transmissivity coefficient 2023

. Fig. 4 Daily variation of transmissivity coefficient at Okhaldhunga in the years 2021, 2022 and 2023

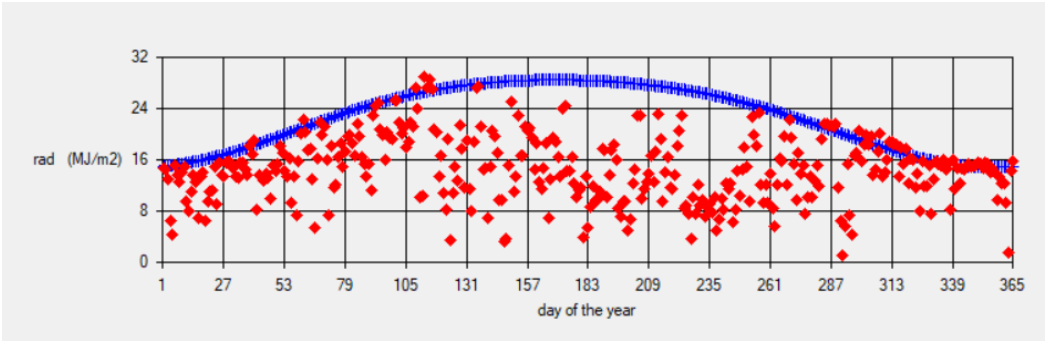

a. Daily variation GSR at for the year 2021

Power System Technology
ISSN:1000-3673
Received: 06-01-2025 Revised: 15-02-2025 Accepted: 25-03-2025

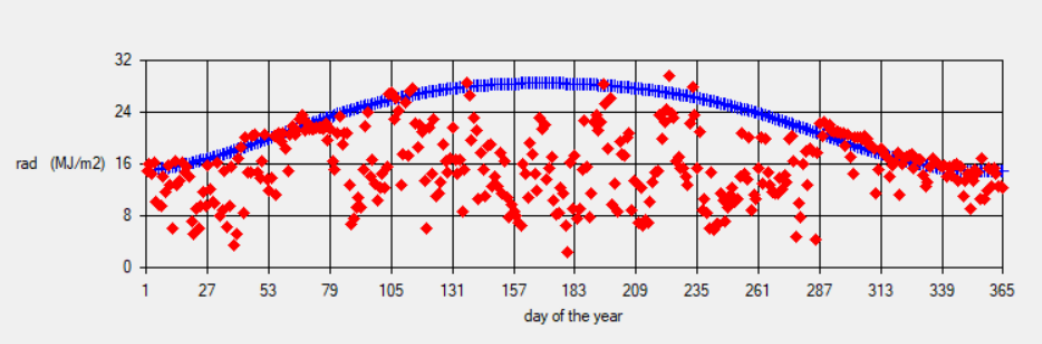

b. Daily variation GSR at Okhaldhunga for the year 2022

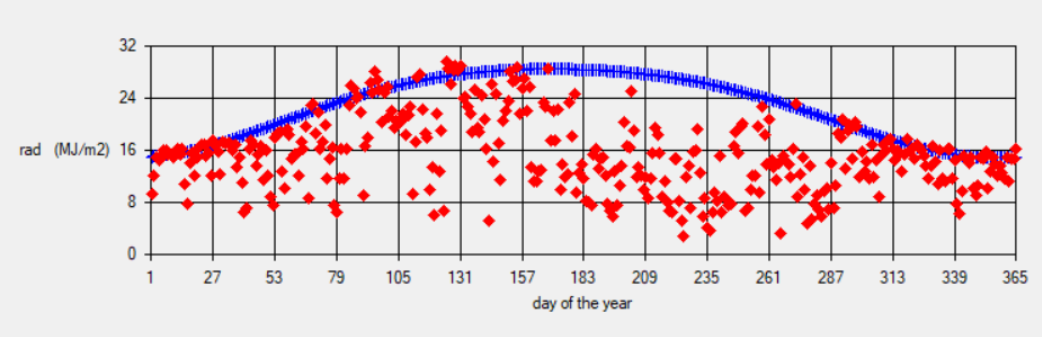

c. Daily variation GSR at Okhaldhunga for the year 2023

Fig. 5 Daily variation GSR at Okhaldhunga for the years 2021, 2022 and 2023

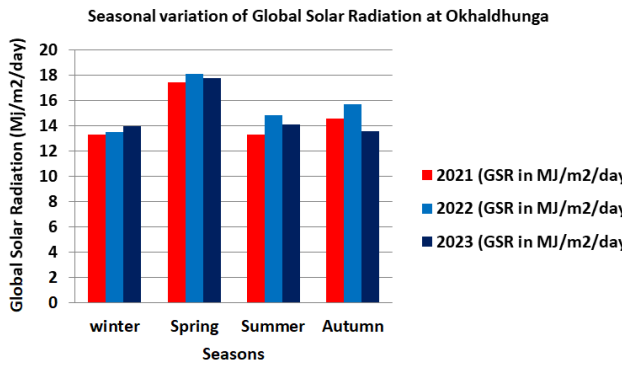

Fig. 6 Seasonal Variation of GSR

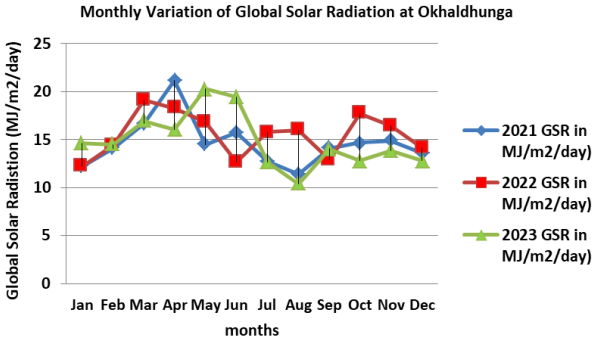

Fig. 7 Monthly Variation of GSR

Power System Technology
ISSN:1000-3673
Received: 06-01-2025 Revised: 15-02-2025 Accepted: 25-03-2025

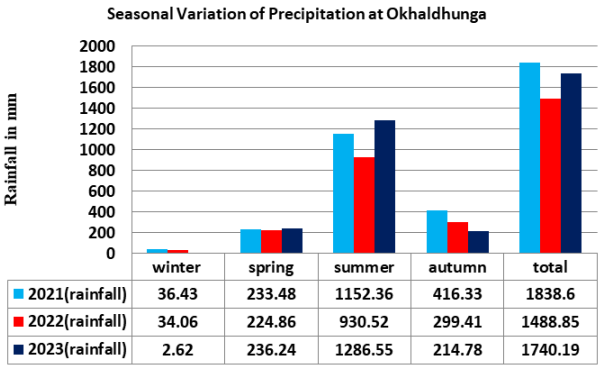

	winter	spring	summer	autumn	total
2021(rainfall)	36.43	233.48	1152.36	416.33	1838.6
2022(rainfall)	34.06	224.86	930.52	299.41	1488.85
2023(rainfall)	2.62	236.24	1286.55	214.78	1740.19

Fig. 8 Seasonal Variation of Precipitation

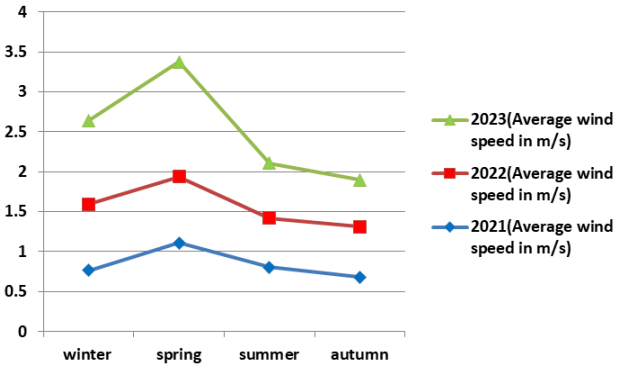

Fig. 9 Seasonal Variation of average wind speed

5 Conclusions

The analysis of Okhaldhunga solar radiation data for the years 2021, 2022, and 2023 reveals that the daily worldwide solar radiation levels are 14.6 ± 0.27 MJ/m^2/day, 15.5 ± 0.27 MJ/m^2/day, and 15.4 ± 0.32 MJ/m^2/day, respectively. This is a significant amount of funding to assist power plants in Okhaldhunga. The intensity of solar radiation varies depending on local meteorological factors such as temperature, humidity, rainfall, wind speed, and daylight hours. On clear sky days, radiation increases after the monsoon due to ground albedo. Therefore, in many areas, the topography and local weather conditions significantly affect the prediction of GSR. In conclusion, Okhaldhunga has significant potential for solar energy utilization, with a solar insolation of 4.31 ± 0.08 kWh/m^2/day. This high insolation results from lower air pollution, precipitation, cloud cover, relative humidity, and south-facing mountains.

In our research analysis, we tested four models using RadEst 3.0. The CD model showed the highest coefficient of determination and the fewest mistakes among the four models, making it the most appropriate for this hilly area. To summarize, the empirical coefficient values of the CD model can be used to calculate solar radiation flow and solar energy in geographic regions like Nepal's.

Acknowledgements

The authors are grateful to the FAOSDRN Agrometeorology Group in Rome, Italy and ISCI-Crop Science in Bologna, Italy for making the RadEst 3.00 software and documentation available for free use in academic settings. They also thank the DHM of the Government of Nepal for providing meteorological data. The authors express their sincere gratitude to everyone who contributed to this study.

Funding: This research was performed independently without financial backing.

Power System Technology
ISSN:1000-3673
Received: 06-01-2025 Revised: 15-02-2025 Accepted: 25-03-2025

Conflict of interest: The authors declare no conflicts of interest.

References

1. WECS. Energy Synopsis Report, 2023. Government of Nepal.
2. Lamsal H. NEA to connect all households with electricity by 2022. Republica.
3. Shrestha JN, Bajracharya TR, Shakya SR, Giri B. Renewable energy in Nepal: progress at a glance from 1998 to 2003. In: Proceedings of the International Conference on Renewable Energy Technology for Rural Development (RETRUD-03). 2003 Oct; 3:12-14.
4. Poudyal KN. Estimation of global solar radiation potential in Nepal [PhD thesis]. IOE, Tribhuvan University; 2015.
5. Joshi U, Poudyal KN, Karki IB, Chapagain NP. Evaluation of global solar radiation using sunshine hour, temperature, and relative humidity at the lowland region of Nepal. J Nepal Phys Soc. 2020 Aug 2;6(1):16-24.
6. GEAW Team. Global energy assessment. Cambridge: Cambridge Books; 2012.
7. Angstrom A. Solar and terrestrial radiation: report to the International Commission for Solar Research on actinometric investigations of solar and atmospheric radiation. Q J R Meteorol Soc. 1924 Apr;50(210):121-6.
8. Iqbal M. An introduction to solar radiation. Elsevier; 2012 Dec 2.
9. Ali MA, Elsayed A, Elkabani I, Akrami M, Youssef ME, Hassan GE. Optimizing artificial neural networks for the accurate prediction of global solar radiation: a performance comparison with conventional methods. Energies. 2023 Aug 24;16(17):6165.
10. Olomiyesan BM, Oyedum OD, Ugwuoke PE, Abolarin MS. Evaluation of some global solar radiation models in selected locations in Northwest Nigeria. Open Access J Photoenergy. 2017;1(1):1-6.
11. Nage GD. Estimation of monthly average daily solar radiation from meteorological parameters: sunshine hours and measured temperature in Tepi, Ethiopia. Int J Energy Environ Sci. 2018 Feb;3(1):19-26.
12. Li H, Cao F, Wang X, Ma W. A temperature-based model for estimating monthly average daily global solar radiation in China. Sci World J. 2014;2014(1):128754.
13. Teyabeen AA, Elhatmi NB, Essnid AA, Mohamed F. Estimation of monthly global solar radiation over twelve major cities of Libya. Energy Built Environ. 2024 Feb 1;5(1):46-57.
14. Hassan GE, Youssef ME, Mohamed ZE, Ali MA, Hanafy AA. New temperature-based models for predicting global solar radiation. Appl Energy. 2016 Oct 1;179:437-50.

Power System Technology
ISSN:1000-3673
Received: 06-01-2025 Revised: 15-02-2025 Accepted: 25-03-2025

15. Narejo KA, Rehman SU, Tariq I, Zahid MM, Sadiq N, Khan MM, Uddin Z. MEP modeled new equations for ASHRAE constant to estimate solar radiation. Indian J Phys. 2024 Feb 22;1-5.
16. Hissou H, Benkirane S, Guezzaz A, Azrour M, Beni-Hssane A. A novel machine learning approach for solar radiation estimation. Sustainability. 2023 Jul 5;15(13):10609.
17. Joshi U, Karki IB, Chapagain NP, Poudyal KN. Prediction of daily global solar radiation using different empirical models on the basis of meteorological parameters at Trans Himalaya Region, Nepal. Nepal BIBECHANA. 2021 Jan 1;18(1):159-69.
18. Dhakal S, Gautam Y, Bhattarai A. Evaluation of temperature-based empirical models and machine learning techniques to estimate daily global solar radiation at Biratnagar Airport, Nepal. Adv Meteorol. 2020;2020(1):8895311.
19. Joshi U, Chapagain NP, Karki IB, Shrestha PM, Poudyal KN. Estimation of daily solar radiation flux at Western Highland, Simikot, Nepal using RadEst 3.0 software. Int J Syst Assur Eng Manag. 2022 Feb;13(1):318-27.
20. Bristow KL, Campbell GS. On the relationship between incoming solar radiation and daily maximum and minimum temperature. Agric For Meteorol. 1984 May 1;31(2):159-66.
21. Donatelli M, Bellocchi G. Estimate of daily global solar radiation: new developments in the software RadEst 3.00. In: Proceedings of the 2nd International Symposium on Modelling Cropping Systems, Florence, Italy. 2001 Jul 16;16-18.
22. Donatelli M, Bellocchi G, Fontana F. RadEst 3.00: software to estimate daily radiation data from commonly available meteorological variables. Eur J Agron. 2003 Jan 1;18(3-4):363-7.
23. Poudyal KN, Bhattarai BK, Sapkota B, Kjeldstad B, Daponte P. Estimation of the daily global solar radiation: Nepal experience. Measurement. 2013 Jul 1;46(6):1807-17.
24. Poudyal KN, Bhattarai BK, Sapkota B, Kjeldstad B. Estimation of the daily global solar radiation using RadEst 3.00 software: a case study at low land plain region of Nepal. J Nepal Chem Soc. 2012;29:48-57.
25. Khatri Chhetri BR, Gurung S. Estimation of total solar radiation using RadEst 3.00 software at Jumla, Nepal. Int J Syst Assur Eng Manag. 2017 Nov;8:1527-33.